Cytochrome P450 Drives a HIF-Regulated Behavioral Response to Reoxygenation by *C. elegans*

Dengke K. Ma,[1] Michael Rothe,[2] Shu Zheng,[1] Nikhil Bhatla,[1] Corinne L. Pender,[1] Ralph Menzel,[3] H. Robert Horvitz[1]*

Oxygen deprivation followed by reoxygenation causes pathological responses in many disorders, including ischemic stroke, heart attacks, and reperfusion injury. Key aspects of ischemia-reperfusion can be modeled by a *Caenorhabditis elegans* behavior, the O2-ON response, which is suppressed by hypoxic preconditioning or inactivation of the O_2-sensing HIF (hypoxia-inducible factor) hydroxylase EGL-9. From a genetic screen, we found that the cytochrome P450 oxygenase CYP-13A12 acts in response to the EGL-9–HIF-1 pathway to facilitate the O2-ON response. CYP-13A12 promotes oxidation of polyunsaturated fatty acids into eicosanoids, signaling molecules that can strongly affect inflammatory pain and ischemia-reperfusion injury responses in mammals. We propose that roles of the EGL-9–HIF-1 pathway and cytochrome P450 in controlling responses to reoxygenation after anoxia are evolutionarily conserved.

Ischemia-reperfusion–related disorders, such as strokes and heart attacks, are the most common causes of adult deaths worldwide (*1*). Blood delivers O_2 and nutrients to target tissues, and ischemia results when the blood supply is interrupted. The restoration of O_2 from blood flow after ischemia, known as reperfusion, can exacerbate tissue damage (*2*). How organisms prevent ischemia-reperfusion injury is poorly understood. Studies of the nematode *C. elegans* led to the discovery of an evolutionarily conserved family of O_2-dependent enzymes (EGL-9 in *C. elegans* and EGLN2 in mammals) that hydroxylate the HIF transcription factor and link hypoxia to hypoxia-inducible factor (HIF)–mediated physiological responses (*3*–*7*). Exposure to chronic low concentrations of O_2 (hypoxic preconditioning) or direct inhibition of EGLN2 strongly protects mammals from stroke and ischemia-reperfusion injury (*2*, *8*, *9*). Similarly, EGL-9 inactivation in *C. elegans* blocks a behavioral response to reoxygenation, the O2-ON response (characterized by a rapidly increased locomotion speed triggered by reoxygenation after anoxia) (*10*, *11*), which is similar to mammalian tissue responses to ischemia-reperfusion: (i) Reoxygenation drives the O2-ON response and is the major pathological driver of reperfusion injury, (ii) hypoxic preconditioning can suppress both processes, and (iii) the central regulators (EGL-9–HIF) of both processes are evolutionarily conserved. It remains unknown how the EGL-9–HIF-1 and EGLN2-HIF pathways control the O2-ON response and ischemia-reperfusion injury, respectively.

To seek EGL-9–HIF-1 effectors important in the O2-ON response, we performed an *egl-9* suppressor screen for mutations that can restore the defective O2-ON response in *egl-9* mutants (fig. S1A). We identified new alleles of *hif-1* in this screen; because EGL-9 inhibits HIF-1, *hif-1* mutations suppress the effects of *egl-9* mutations (*10*). We also identified mutations that are not alleles of *hif-1* (Fig. 1, A to C, and fig. S1B). *hif-1* mutations recessively suppressed three defects of *egl-9* mutants: the defective O2-ON response, defects in egg laying, and the ectopic expression of the HIF-1 target gene *cysl-2* (previously called *K10H10.2*) (fig. S1C) (*10*, *12*). By contrast, one mutation, *n5590*, dominantly suppressed the O2-ON defect but did not suppress the egg-laying defect or the ectopic expression of *cysl-2::GFP* (Fig. 1, D and E, and fig. S2). *n5590* restored the sustained phase (starting 30 s after reoxygenation) better than it did the initial phase (within 30 s after reoxygenation) (Fig. 1, A to C). *egl-9*; *hif-1*; *n5590* triple mutants displayed a normal O2-ON response, just like the wild type and *egl-9*; *hif-1* double mutants (fig. S1D). Thus, *n5590* specifically suppresses the *egl-9* defect in the sustained phase of the O2-ON response.

We genetically mapped *n5590* and identified a $Met^{46} \rightarrow Ile$ missense mutation in the gene *cyp-13A12* by whole-genome sequencing (Fig. 2A, fig. S3A, and table S1A). Decreased wild-type *cyp-13A12* gene dosage in animals heterozygous for a wild-type allele and the splice acceptor null mutation *gk733685*, which truncates the majority of the protein, did not recapitulate the dominant effect of *n5590* (Fig. 2B). Similarly, *gk733685* homozygous mutants did not recapitulate the effect of *n5590* (Fig. 2C). Thus, *n5590* does not cause a loss of gene function. By contrast, increasing wild-type *cyp-13A12* gene dosage by overexpression restored the sustained phase of the O2-ON response (Fig. 2D), and RNA interference (RNAi) against *cyp-13A12* abolished the effect of *n5590* (Fig. 2E). We conclude that *n5590* is a gain-of-function allele of *cyp-13A12*.

cyp-13A12 encodes a cytochrome P450 oxygenase (CYP). CYPs can oxidize diverse substrates (*13*–*15*). The *C. elegans* genome contains about 82 CYP genes, at least two of which are polyunsaturated fatty acid (PUFA) oxygenases that generate eicosanoid signaling molecules (fig. S3B) (*16*, *17*). On the basis of BLASTP scores, the closest human homolog of CYP-13A12 is CYP3A4 (fig. S4). We aligned the protein sequences of CYP-13A12 and CYP3A4 and found that *n5590* converts methionine 46 to an isoleucine, the residue in the corresponding position of normal human CYP3A4 (fig. S4). Methionines can be oxidized by free radicals, which are produced in the CYP enzymatic cycle, rendering CYPs prone to degradation (*18*, *19*). Using transcriptional and translational green fluorescent protein (GFP)–based reporters, we identified the pharyngeal marginal cells as the major site of expression of *cyp-13A12* (fig. S5) and observed that the abundance of CYP-13A12::GFP protein was decreased by prolonged hypoxic preconditioning and also decreased in *egl-9* but not in *egl-9*; *hif-1* mutants (Fig. 2F and fig. S5). The *n5590* mutation prevented the decrease in CYP-13A12::GFP abundance by hypoxia or *egl-9*. Thus, *n5590* acts, at least in part, by restoring the normal abundance of CYP-13A12, which then promotes the O2-ON response in *egl-9* mutants.

We tested whether CYP-13A12 was normally required for the O2-ON response in wild-type animals. The *cyp-13A12* null allele *gk733685* abolished the sustained phase of the O2-ON response; the initial phase of the O2-ON response was unaffected (Fig. 3A). A wild-type *cyp-13A12* transgene fully rescued this defect (Fig. 3B). A primary role of CYP-13A12 in the sustained phase of the O2-ON response explains the incomplete rescue of the defective O2-ON response of *egl-9* mutants by *n5590* during the initial phase (Fig. 1C). The activity of most and possibly all *C. elegans* CYPs requires EMB-8, a CYP reductase that transfers electrons to CYPs (*20*). No non-CYP EMB-8 targets are known. The mutation *emb-8(hc69)* causes a temperature-sensitive embryonic lethal phenotype. We grew *emb-8(hc69)* mutants at the permissive temperature to the young-adult stage. A shift to the nonpermissive temperature simultaneously with *Escherichia coli*–feeding RNAi against *emb-8* nearly abolished the O2-ON response (Fig. 3, C and D). [Both the *hc69* mutation and RNAi against *emb-8* were required to substantially reduce the level of EMB-8 (*17*).] CYP-13A12 is thus required for the sustained phase of the O2-ON response, and one or more other CYPs likely act with CYP-13A12 to control both phases of the O2-ON response.

CYP oxygenases define one of three enzyme families that can convert PUFAs to eicosanoids, which are signaling molecules that affect inflam-

[1]Howard Hughes Medical Institute, Department of Biology, McGovern Institute for Brain Research, Koch Institute for Integrative Cancer Research, Massachusetts Institute of Technology, Cambridge, MA 02139, USA. [2]Lipidomix GmbH, Robert-Roessle-Str. 10, 13125 Berlin, Germany. [3]Freshwater and Stress Ecology, Department of Biology, Humboldt-Universität zu Berlin, Spaethstr. 80/81, 12437 Berlin, Germany.

*Corresponding author. E-mail: horvitz@mit.edu

matory pain and ischemia-reperfusion responses of mammals (*15*, *21*–*23*); the other two families, cyclooxygenases and lipoxygenases, do not appear to be present in *C. elegans* (*17*, *24*). To test whether eicosanoids are regulated by EGL-9 and CYP-13A12, we used high-performance liquid chromatography (HPLC) coupled with mass spectrometry (MS) to profile steady-state amounts of 21 endogenous eicosanoid species from cell extracts of wild-type, *egl-9(n586)*, and *egl-9(n586); cyp-13A12(n5590)* strains. Only free eicosanoids have potential signaling roles (*21*, *22*, *24*), so we focused on free eicosanoids. The *egl-9* mutation caused a marked decrease in the overall amount of free eicosanoids, whereas the total amount of eicosanoids, including both free and membrane-bound fractions, was unaltered (Fig. 4A and fig. S6). Among the eicosanoids profiled, 17,18-DiHEQ (17,18-diolhydroxyeicosatetraenoic acid) was the most abundant species (fig. S6B). 17,18-DiHEQ is the catabolic hydrolase product of 17,18-EEQ (17,18-epoxyeicosatetraenoic acid), an epoxide active in eicosanoid signaling (*25*). Free cytosolic 17,18-EEQ and 19-hydroxyeicosatetraenoic acid (19-HETE) were present in the wild type but undetectable in *egl-9* mutants (Fig. 4, C to F). *egl-9(n586)*; *cyp-13A12(n5590)* mutants exhibited partially restored free overall eicosanoid levels as well as restored levels of 17,18-EEQ and 19-HETE (Fig. 4, A to F, and fig. S6B). Thus, both EGL-9 and CYP-13A12 regulate amounts of free cytosolic eicosanoids.

We tested whether the O2-ON response requires PUFAs, which are CYP substrates and eicosanoid precursors. PUFA-deficient *fat-2* and *fat-3* mutants (*26*) exhibited a complete lack of the O2-ON response, although the acceleration in response to anoxia preceding the O2-ON response was normal (Fig. 4G and fig. S7, A to C). The defective O2-ON response of *fat-2* mutants was restored by feeding animals arachidonic acid, a C20 PUFA (Fig. 4H), but not oleate, a C18 monounsaturated fatty acid that is processed by FAT-2 to generate C20 PUFAs (fig. S7D). These results demonstrate an essential role of PUFAs for the O2-ON response.

We suggest a model in which CYPs, which are strictly O_2-dependent (*27*, *28*), generate eicosanoids to drive the O2-ON response (Fig. 4I and fig. S8). In this model, EGL-9 acts as a chronic O_2 sensor, so that during hypoxic preconditioning, the O_2-dependent activity of EGL-9 is inhibited, HIF-1 is activated, and unknown HIF-1 up-regulated targets decrease CYP protein abundance. The low abundance of CYPs defines the hypoxic preconditioned state. Without hypoxic preconditioning, CYPs generate eicosanoids, which drive the O2-ON response. By contrast, with hypoxic preconditioning or in *egl-9* mutants, the CYP amounts are insufficient to generate eicosanoids and the O2-ON response is not triggered. Neither C20 PUFAs nor overexpression of CYP-29A3 restored the defective O2-ON response of *egl-9* mutants (figs. S9 and S10), indicating that this defect is unlikely to be caused by a general deficiency in C20 PUFAs or CYPs. Because the O2-ON response requires EMB-8, a general CYP reductase, but only the sustained phase requires CYP-13A12, we propose

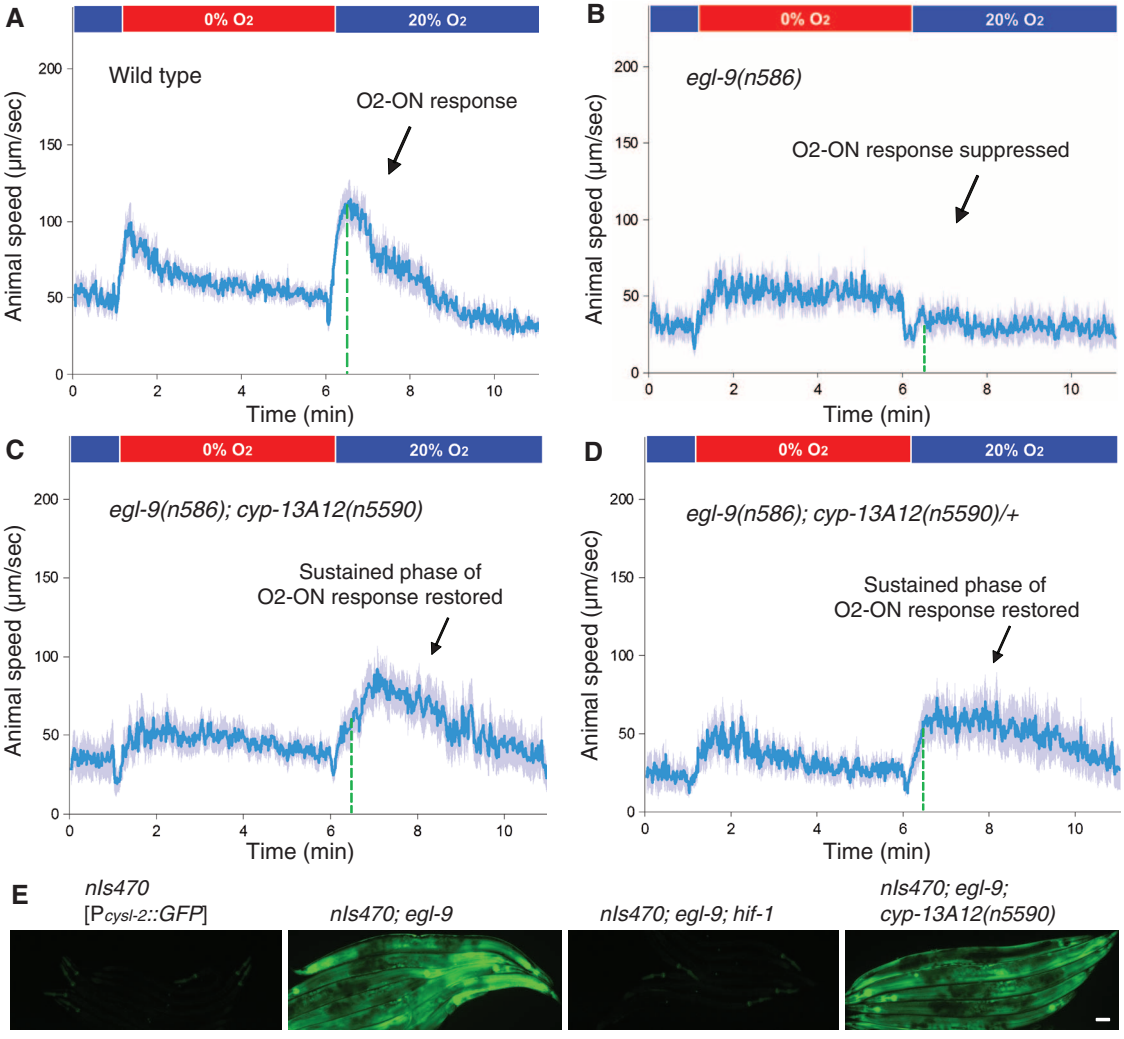

Fig. 1. *n5590* suppresses the defect of *egl-9* mutants in the O2-ON response. (**A**) Speed graph of wild-type animals, showing a normal O2-ON response. Average speed values ± 2 SEM (blue) of animals ($n > 50$) are shown with step changes of O_2 between 20 and 0% at the indicated times. The mean speed within 0 to 120 s after O_2 restoration is increased relative to that before O_2 restoration ($P < 0.01$, one-sided unpaired *t* test). The dashed green line indicates the approximate boundary (30 s after reoxygenation) between the initial and sustained phases of the O2-ON response. (**B**) Speed graph of *egl-9(n586)* mutants, showing a defective O2-ON response. (**C**) Speed graph of *egl-9(n586)*; *cyp-13A12(n5590)* mutants, showing a restored O2-ON response mainly in the sustained phase (right of the dashed green line). The mean speed within 30 to 120 s after O_2 restoration was significantly higher than that of *egl-9(n586)* mutants ($P < 0.01$). (**D**) Speed graph of *egl-9(n586)*; *cyp-13A12(n5590)/+* mutants, showing a restored O2-ON response in the sustained phase. (**E**) *hif-1* but not *cyp-13A12 (n5590)* suppressed the expression of *cysl-2::GFP* by *egl-9(n586)* mutants. GFP fluorescence micrographs of five to seven worms aligned side by side carrying the transgene *nIs470 [P_{cysl-2}::GFP]* are shown. Scale bar, 50 µm.

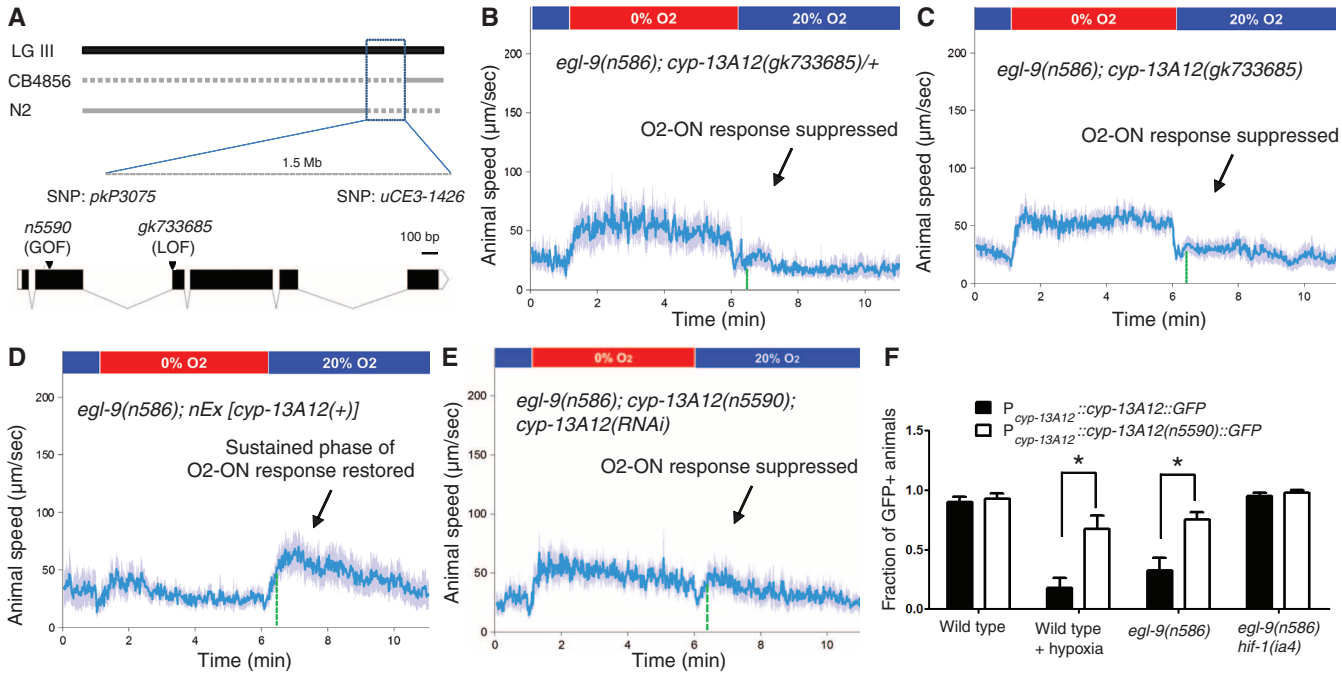

Fig. 2. *n5590* is a gain-of-function allele of *cyp-13A12*. (**A**) Genetic mapping positioned *n5590* between the SNPs *pkP3075* and *uCE3-1426*. Solid gray lines indicate genomic regions for which recombinants exhibited a defective O2-ON response, thus excluding *n5590* from those regions. The locations of *n5590* and *gk733685* are indicated in the gene diagram of *cyp-13A12*. (**B**) Speed graph of *egl-9(n586)*; *cyp-13A12(gk733685)/+* animals, showing a defective O2-ON response. (**C**) Speed graph of *egl-9(n586); cyp-13A12(gk733685)* mutants, showing a defective O2-ON response. (**D**) Speed graph *of egl-9(n586)*; *nEx [cyp-13A12(+)]* animals, showing a restored O2-ON response in the sustained phase (right of the dashed green line). (**E**) Speed graph of *egl-9(n586)*; *cyp-13A12(n5590)*; *cyp-13A12(RNAi)* animals, showing a suppressed O2-ON response. (**F**) Fractions of animals expressing CYP-13A12::GFP or CYP-13A12(*n5590*)::GFP [*$P < 0.01$, two-way analysis of variance (ANOVA) with Bonferroni test, $n = 4$].

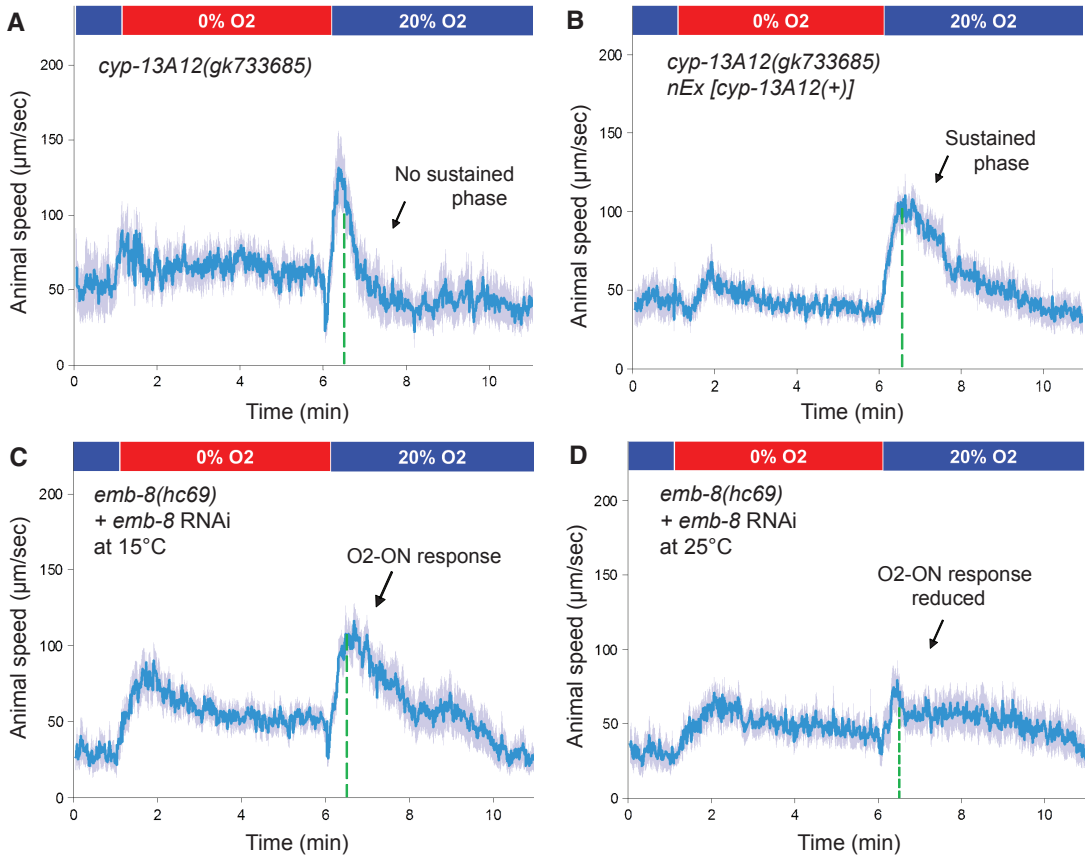

Fig. 3. Requirement of CYP-13A12 for a normal O2-ON response. (**A**) Speed graph of *cyp-13A12(gk733685)* loss-of-function mutants, showing an O2-ON response with a normal initial phase but a diminished sustained phase (left and right, respectively, of the dashed green line). (**B**) Speed graph of *cyp-13A12(gk733685)* mutants with a rescuing wild-type *cyp-13A12* transgene, showing the O2-ON response with a normal initial phase and sustained phase. The mean speed within 30 to 120 s after O_2 restoration was higher than that of *cyp-13A12(gk733685)* mutants ($P < 0.01$, one-sided unpaired *t* test, $n > 50$). (**C**) Speed graph of *emb-8(hc69)* mutants grown at the permissive temperature of 15°C with simultaneous *E. coli*–feeding RNAi against *emb-8*, showing a normal O2-ON response. (**D**) Speed graph of *emb-8(hc69)* mutants grown post-embryonically at the restrictive temperature of 25°C with simultaneous *E. coli*–feeding RNAi against *emb-8*, showing a reduced O2-ON response.

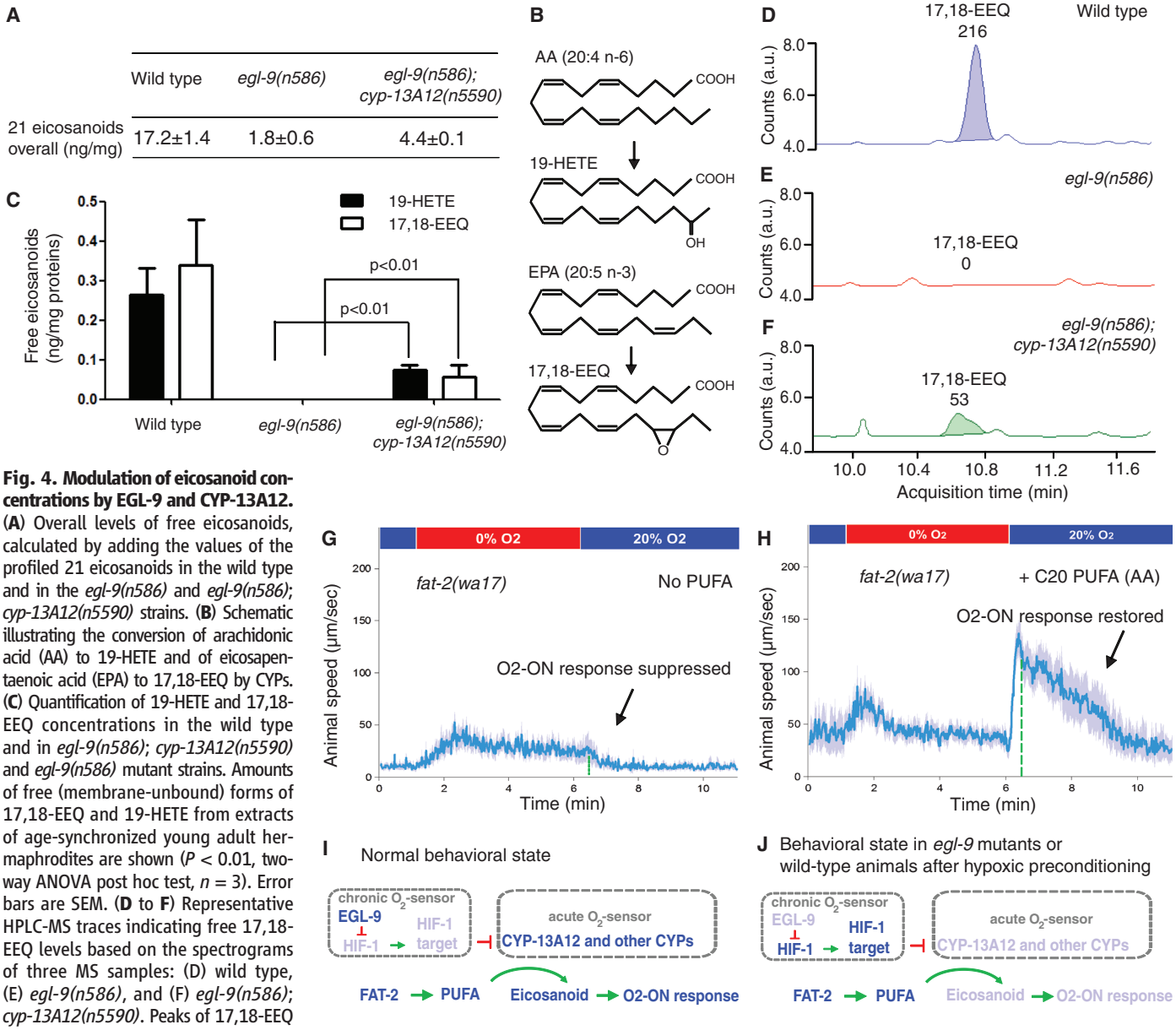

Fig. 4. Modulation of eicosanoid concentrations by EGL-9 and CYP-13A12. (**A**) Overall levels of free eicosanoids, calculated by adding the values of the profiled 21 eicosanoids in the wild type and in the *egl-9(n586)* and *egl-9(n586); cyp-13A12(n5590)* strains. (**B**) Schematic illustrating the conversion of arachidonic acid (AA) to 19-HETE and of eicosapentaenoic acid (EPA) to 17,18-EEQ by CYPs. (**C**) Quantification of 19-HETE and 17,18-EEQ concentrations in the wild type and in *egl-9(n586)*; *cyp-13A12(n5590)* and *egl-9(n586)* mutant strains. Amounts of free (membrane-unbound) forms of 17,18-EEQ and 19-HETE from extracts of age-synchronized young adult hermaphrodites are shown ($P < 0.01$, two-way ANOVA post hoc test, $n = 3$). Error bars are SEM. (**D** to **F**) Representative HPLC-MS traces indicating free 17,18-EEQ levels based on the spectrograms of three MS samples: (D) wild type, (E) *egl-9(n586)*, and (F) *egl-9(n586); cyp-13A12(n5590)*. Peaks of 17,18-EEQ at its transition *m/z* (mass-to-charge ratio) were measured and extracted (MassHunter). The *x* axis shows the retention time (minutes); the *y* axis shows the abundance (counts), with specific integral values over individual peaks indicated above each peak. (**G**) Speed graph of *fat-2* mutants, showing a defective O2-ON response. Animals were supplemented with the solvents used in (H) as a control. (**H**) Speed graph of *fat-2* mutants, showing the O2-ON response rescued by C20 PUFA (AA) supplementation. (**I** and **J**) Model of how EGL-9 and CYPs control the O2-ON response under (I) normoxic conditions and (J) conditions of hypoxic preconditioning or in *egl-9* mutants (see text for details). Light blue indicates low protein activity, low amounts of eicosanoids, or a defective O2-ON response.

that CYP-13A12 and other CYPs act as acute O_2 sensors and produce eicosanoids, which are short-lived and act locally (*22*) during reoxygenation to signal nearby sensory circuits that drive the O2-ON response.

In humans, a low uptake of PUFAs or an imbalanced ratio of ω3-to-ω6 PUFAs is associated with elevated risk of stroke, cardiovascular disease, and cancer (*21*, *23*, *29*, *30*). Cytochrome P450s and eicosanoid production also have been implicated in mammalian ischemia-reperfusion (*15*, *21*). Nonetheless, little is known concerning the causal relationships among and mechanisms relating O_2 and PUFA homeostasis, CYP, and PUFA-mediated cell signaling and organismal susceptibility to oxidative disorders. Our results identify a pathway in which EGL-9–HIF-1 regulates CYP-eicosanoid signaling, demonstrate that PUFAs confer a rapid response to reoxygenation via CYP-generated eicosanoids, and provide direct causal links among CYPs, PUFA-derived eicosanoids, and an animal behavioral response to reoxygenation. Because the molecular mechanisms of O_2 and PUFA homeostasis are fundamentally similar and evolutionarily conserved between nematodes and mammals (*7*, *11*, *26*), we suggest that the *C. elegans* O2-ON response is analogous to the mammalian tissue and cellular response to ischemia-reperfusion injury and that the molecular pathway including EGL-9–HIF-1 and CYPs in controlling responses to reoxygenation after anoxia is evolutionarily conserved.

References and Notes

1. A. S. Go *et al.*, *Circulation* **127**, e6–e245 (2013).
2. H. K. Eltzschig, T. Eckle, *Nat. Med.* **17**, 1391–1401 (2011).
3. A. C. Epstein *et al.*, *Cell* **107**, 43–54 (2001).
4. W. G. Kaelin Jr., P. J. Ratcliffe, *Mol. Cell* **30**, 393–402 (2008).
5. C. Trent, N. Tsuing, H. R. Horvitz, *Genetics* **104**, 619–647 (1983).
6. G. L. Semenza, *Cell* **148**, 399–408 (2012).
7. J. A. Powell-Coffman, *Trends Endocrinol. Metab.* **21**, 435–440 (2010).

8. G. L. Semenza, *Biochim. Biophys. Acta* **1813**, 1263–1268 (2011).
9. J. Aragonés *et al.*, *Nat. Genet.* **40**, 170–180 (2008).
10. D. K. Ma, R. Vozdek, N. Bhatla, H. R. Horvitz, *Neuron* **73**, 925–940 (2012).
11. D. K. Ma, N. Ringstad, *Front. Biol.* **7**, 246–253 (2012).
12. M. W. Budde, M. B. Roth, *Genetics* **189**, 521–532 (2011).
13. D. R. Nelson *et al.*, *Pharmacogenetics* **6**, 1–42 (1996).
14. O. Gotoh, *Mol. Biol. Evol.* **15**, 1447–1459 (1998).
15. R. A. Gottlieb, *Arch. Biochem. Biophys.* **420**, 262–267 (2003).
16. M. Kosel *et al.*, *Biochem. J.* **435**, 689–700 (2011).
17. J. Kulas, C. Schmidt, M. Rothe, W. H. Schunck, R. Menzel, *Arch. Biochem. Biophys.* **472**, 65–75 (2008).
18. B. S. Berlett, E. R. Stadtman, *J. Biol. Chem.* **272**, 20313–20316 (1997).
19. R. C. Zangar, D. R. Davydov, S. Verma, *Toxicol. Appl. Pharmacol.* **199**, 316–331 (2004).
20. C. A. Rappleye, A. Tagawa, N. Le Bot, J. Ahringer R. V. Aroian, *BMC Dev. Biol.* **3**, 8 (2003).
21. J. Szefel *et al.*, *Curr. Mol. Med.* **11**, 13–25 (2011).
22. M. P. Wymann, R. Schneiter, *Nat. Rev. Mol. Cell Biol.* **9**, 162–176 (2008).
23. R. S. Chapkin, W. Kim, J. R. Lupton, D. N. McMurray, *Prostaglandins Leukot. Essent. Fatty Acids* **81**, 187–191 (2009).
24. D. Panigrahy, A. Kaipainen, E. R. Greene, S. Huang, *Cancer Metastasis Rev.* **29**, 723–735 (2010).
25. C. Arnold *et al.*, *J. Biol. Chem.* **285**, 32720–32733 (2010).
26. J. L. Watts, *Trends Endocrinol. Metab.* **20**, 58–65 (2009).
27. D. R. Harder *et al.*, *Circ. Res.* **79**, 54–61 (1996).
28. J. P. Ward, *Biochim. Biophys. Acta* **1777**, 1–14 (2008).
29. M. Gerber, *Br. J. Nutr.* **107** (suppl. 2), S228–S239 (2012).
30. D. Mozaffarian, J. H. Wu, *J. Am. Coll. Cardiol.* **58**, 2047–2067 (2011).

Acknowledgments: We thank C. Bargmann, A. Fire, A. Hart, Y. Iino, J. Powell-Coffman, and C. Rongo for reagents and the *Caenorhabditis* Genetics Center and the Million Mutation Project for strains. H.R.H. is an Investigator of the Howard Hughes Medical Institute. Supported by NIH grant GM24663 (H.R.H), German Research Foundation grant ME2056/3-1 (R.M.), a NSF Graduate Research Fellowship (N.B.), the MIT Undergraduate Research Opportunities Program (S.Z.), and a Helen Hay Whitney Foundation postdoctoral fellowship (D.K.M.).

Supplementary Materials

www.sciencemag.org/cgi/content/full/science.1235753/DC1
Materials and Methods
Supplementary Text
Figs. S1 to S11
Table S1
References (*31*–*70*)

28 January 2013; accepted 10 June 2013
Published online 27 June 2013;
10.1126/science.1235753

Robustness and Compensation of Information Transmission of Signaling Pathways

Shinsuke Uda,[1] Takeshi H Saito,[1] Takamasa Kudo,[1] Toshiya Kokaji,[2] Takaho Tsuchiya,[1] Hiroyuki Kubota,[1] Yasunori Komori,[1] Yu-ichi Ozaki,[1]* Shinya Kuroda[1,2,3]†

Robust transmission of information despite the presence of variation is a fundamental problem in cellular functions. However, the capability and characteristics of information transmission in signaling pathways remain poorly understood. We describe robustness and compensation of information transmission of signaling pathways at the cell population level. We calculated the mutual information transmitted through signaling pathways for the growth factor–mediated gene expression. Growth factors appeared to carry only information sufficient for a binary decision. Information transmission was generally more robust than average signal intensity despite pharmacological perturbations, and compensation of information transmission occurred. Information transmission to the biological output of neurite extension appeared robust. Cells may use information entropy as information so that messages can be robustly transmitted despite variation in molecular activities among individual cells.

Signaling pathways transmit signals from growth factors to downstream gene expression, influencing various cell fate decisions such as cell differentiation (*1*). To control cellular responses by stimulation intensity, signaling pathways must reliably transmit stimulation intensity through their signaling activities. The reliability of signal transmission depends on the balance between signal intensity and variation. The smaller the signal variation, the more information can be transmitted through a pathway with the same dynamic range of signal intensity. Even high-intensity signals cannot be reliably transmitted if the variation in signal intensity is large. In contrast, even signals with low intensity can be reliably transmitted if the variation in signal intensity is small (Fig. 1A). Thus, the reliability of signal transmission depends on both average (mean) intensity and variation. As a consequence, the number of controllable states of cellular responses is determined by the number of reliably transmitted signals. Intuitively, the larger the number of reliably transmitted signals, the more information the signal pathway can transmit. If cellular signaling pathways are treated as communication channels in the framework of Shannon's information theory (*2*–*12*), the amount of information that can be reliably transmitted through a cellular signaling pathway can be measured by mutual information, which corresponds to the logarithm of the average number of controllable states of a cellular response that can be defined by varied upstream signals (*13*–*15*).

We evaluated the information transmission from growth factors to the immediate early genes (IEGs) through various signaling pathways in PC12 cells. Nerve growth factor (NGF), pituitary

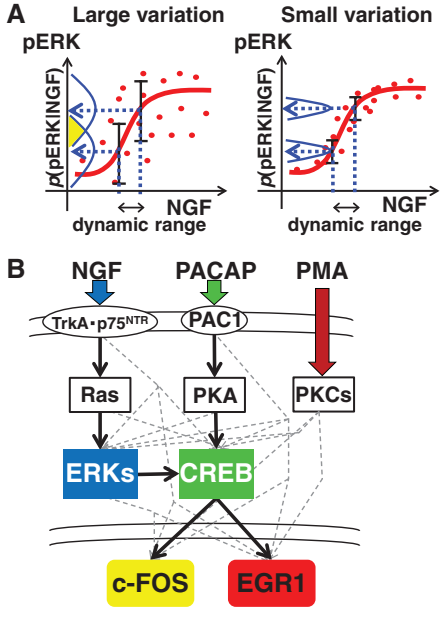

Fig. 1. Information transmission of signaling pathways. (**A**) Reliability of information transmission depends on both signal intensity and variation. More information can be transmitted with the same dynamic range of signal intensity if signal variation is smaller. Dots denote intensities of pERKs in individual cells, and lines denote the average intensity of pERKs. *p*(pERKs|NGF) denotes the distribution (a normalized histogram) of pERKs for a given dose of NGF. (**B**) Signaling pathways from growth factors, such as NGF, PACAP, and PMA to the IEGs, such as c-FOS and EGR1. Solid lines indicate the reported pathways for each growth factor, and gray dashed lines indicate other possible pathways. The colored boxes are the measured molecules, and white ovals are unmeasured molecules in this study.

[1]Department of Biophysics and Biochemistry, Graduate School of Science, University of Tokyo, Bunkyo-ku, Tokyo 113-0033, Japan. [2]Department of Computational Biology, Graduate School of Frontier Sciences, University of Tokyo, Bunkyo-ku, Tokyo 113-0033, Japan. [3]CREST, Japan Science and Technology Corporation, Bunkyo-ku, Tokyo 113-0033, Japan.

*Present address: Quantitative Biology Center, RIKEN, 6-2-3, Furuedai, Suita, Osaka 565-0874, Japan.
†Corresponding author. E-mail: skuroda@bi.s.u-tokyo.ac.jp